Superconvergence of partially penalized immersed finite element methods

HAILONG GUO†, AND XU YANG‡

DEPARTMENT OF MATHEMATICS, UNIVERSITY OF CALIFORNIA,
SANTA BARBARA, CA 93106, USA

AND

ZHIMIN ZHANG§

BEIJING COMPUTATIONAL SCIENCE RESEARCH CENTER,
BEIJING 100193, CHINA
DEPARTMENT OF MATHEMATICS, WAYNE STATE UNIVERSITY,
DETROIT, MI 48202, USA

The contribution of this paper contains two parts: first, we prove a supercloseness result for the partially penalized immersed finite element (PPIFE) methods in [T. Lin, Y. Lin, and X. Zhang, SIAM J. Numer. Anal., 53 (2015), 1121–1144]; then based on the supercloseness result, we show that the gradient recovery method proposed in our previous work [H. Guo and X. Yang, J. Comput. Phys., 338 (2017), 606-619] can be applied to the PPIFE methods and the recovered gradient converges to the exact gradient with a superconvergent rate $\mathscr{O}(h^{1.5})$. Hence, the gradient recovery method provides an asymptotically exact *a posteriori* error estimator for the PPIFE methods. Several numerical examples are presented to verify our theoretical results.

Keywords: superconvergence, interface problem, immersed finite element, supercloseness, gradient recovery.

1. Introduction

Recently there has been of great interest in developing finite element method for interface problems where the discontinuous coefficients appear naturally due to the background consisting of rather different materials; see, e.g.,(Bastian & Engwer, 2009; Babuška, 1970; Barrett & Elliott, 1987; Bramble & King, 1996; Cai & Zhang, 2009; Chen & Dai, 2002; Chen & Zou, 1998; Gong *et al.*, 0708; Hansbo & Hansbo, 2002; Hou & Liu, 2005; Hou *et al.*, 2004; Huang *et al.*, 2017; Li, 1998; Li *et al.*, 2004, 2003; Li & Ito, 2006; Lin *et al.*, 2015; Xu, 1982). It is well known that classical finite element method works for interface problems provided that the mesh is aligned with the interface (Babuška, 1970; Bramble & King, 1996; Chen & Zou, 1998; Xu, 1982). Such requirement may be a heavy burden especially when the interface involves complex geometry and therefore it is difficult and time-consuming to generate a body-fitted mesh. To release the restriction, Li proposed an immersed finite element (IFE) method for the two-point boundary value problem (Li, 1998). This idea was further generalized into two-dimensional cases by Li, Lin, and Wu who constructed a nonconforming IFE method for interface

---

†Email: hlguo@math.ucsb.edu
‡Email: xuyang@math.ucsb.edu
§Corresponding author. Email: zmzhang@csrc.ac.cn, zzhang@math.wayne.edu

problems (Li *et al.*, 2003). The main idea of IFE is to solve interface problems on the Cartesian mesh (uniform mesh) by modifying basis functions near the interface.

The optimal approximation capability of IFE space was justified in (Li *et al.*, 2004). However, there is no proof for the optimal convergence of the classical IFE method in the two-dimensional setting, see (Lin *et al.*, 2015), even though plentiful numerical experiments showed optimal convergence for elliptic equations. Interested readers are referred to (Chou *et al.*, 2010; He *et al.*, 2012; Kwak *et al.*, 2010) for the progress of theoretical results. Moreover, numerical test results demonstrated that classic IFE method (Ji *et al.*, 2014) achieves only the first order convergence in the L^∞ norm. In fact, the error function $|u - u_h|$ has relatively larger values over interfaces due to the discontinuities of both trial and test functions. To eliminate this disadvantage, the authors of (Ji *et al.*, 2014) added a correction term into the bilinear form of the classic IFE method and (Hou & Liu, 2005; Hou *et al.*, 2013, 2004) proposed a new IFE formulation in the framework of the Petrov-Galerkin method, where the test function may not be the trial function. However, the theoretical foundation of their methods is not fully established. Alternatively, Lin, Lin, and Zhang (Lin *et al.*, 2015) proposed PPIFE methods to penalize the inter-element discontinuity. Thanks to the added penalty term, the authors proved the coercivity of the bilinear form and showed the optimal convergence in the energy norm.

Superconvergence is an active research topic in the finite element community and its theory for smooth problems is well established, see, e.g., (Babuška & Strouboulis, 2001; Bank & Xu, 2003; Chen, 2001; Chen & Xu, 2007; Lakhany *et al.*, 2000; Guo & Zhang, 2015; Guo *et al.*, 2017; Lin & Yan, 1996; Naga & Zhang, 2004, 2005; Wahlbin, 1995; Wu & Zhang, 2007; Xu & Zhang, 2004; Zhang & Naga, 2005; Zienkiewicz & Zhu, 1992a,b; Zhu & Lin, 1989), and references therein. On the other hand, however, the superconvergence phenomena for interface problems is not yet well understood due to discontinuing of the coefficient crossing the interface. In (Wei *et al.*, 2014), a supercloseness result between the linear finite element solution and the linear interpolation of the exact solution is proved for a two-dimensional interface problem with a body-fitted mesh. Recently, the first two authors proposed an improved polynomial preserving recovery (IPPR) for interface problem and proved the superconvergence on both mildly unstructured mesh and adaptively refined mesh (Guo & Yang, 2016a). For IFE method, Chou et al. introduced two special interpolation formula to recover flux more accurately for the one-dimensional linear and quadratic IFE elements (Chou, 2012; Chou & Attanayake, 2017). In (Cao *et al.*, 2015), Cao et al. investigated nodal superconvergence phenomena using generalized orthogonal polynomial in the one-dimensional setting. For the two-dimensional case, the first two authors proposed a new gradient recovery technique (Guo & Yang, 2017) for symmetric and consistent IFE method (Ji *et al.*, 2014) and Petrov-Galerkin IFE method (Hou & Liu, 2005; Hou *et al.*, 2013, 2004) and numerically verified its superconvergence. In addition, (Guo & Yang, 2017) numerically showed supercloseness results for both symmetric and consistent IFE method and Petrov-Galerkin IFE method.

The main goal of this work is to establish a complete superconvergence theory for the PPIFE method (Lin *et al.*, 2015). Our analysis relies on the following three key observations: 1) the solution is piecewise smooth on each sub-domain despite of its low global regularity; 2) the basis functions on non-interface elements are just basis functions for the standard linear finite element method; 3) the number of interface elements is roughly $\mathcal{O}(h^{-1})$. The above three observations motivate us to divide elements into the following three disjoint types: interior elements, exterior elements, and interface elements. We can obtain the supercloseness using well-known results in (Bank & Xu, 2003; Chen & Xu, 2007; Xu & Zhang, 2004) on the interior and exterior elements, respectively. In addition, the trace inequalities for the IFE functions in (Lin *et al.*, 2015) and the third observation enables us to establish $\mathcal{O}(h^{1.5})$ supercloseness result for interface elements. Our supercloseness result reduces to the standard one as in (Bank & Xu, 2003; Chen & Xu, 2007; Xu & Zhang, 2004) when the discontinuity disappears. It is

consistent with the fact that the IFE methods become the standard linear finite element method when the discontinuity disappears. Furthermore, we show that the gradient recovery method in (Guo & Yang, 2017) can also be applied to the PPIFE methods. The recovered gradient is proven to be superconvergent to the exact gradient of the interface problem, and therefore, it provides an asymptotically exact *a posterior* error estimator for PPIFE methods.

The rest of the paper is organized as follows. In Section 2, we introduce the model interface problem and the PPIFE methods. In Section 3, we first establish the supercloseness between gradients of the PPIFE solution and the exact solution to the interface problem, and then based on the supercloseness, we prove that the recovered gradient using the method in (Guo & Yang, 2017) is superconvergent to the exact gradient, and hence provides an asymptotically exact *a posteriori* error estimator for PPIFE methods. In Section 4, we present some numerical experiments to support our theoretical results. Finally, we make some conclusive remarks in Section 5.

2. Preliminary

In this section, we shall introduce the elliptic interface problem, and its discrete form using the PPIFE methods(Lin *et al.*, 2015).

2.1 *Elliptic interface problem*

Let Ω be a bounded polygonal domain with Lipschitz boundary $\partial\Omega$ in $\mathbb{R}^2$. A C^2-curve Γ divides Ω into two disjoint subdomains Ω^- and Ω^+, which is typically characterized by zero level set of some level set function ϕ (Osher & Fedkiw, 2003; Sethian, 1996), with $\Omega^- = \{z \in \Omega | \phi(z) < 0\}$ and $\Omega^+ = \{z \in \Omega | \phi(z) > 0\}$. We shall consider the following elliptic interface problem

$$-\nabla \cdot (\beta(z)\nabla u(z)) = f(z), \quad z \text{ in } \Omega \setminus \Gamma, \tag{2.1}$$

$$u = 0, \qquad z \text{ on } \partial\Omega, \tag{2.2}$$

where the diffusion coefficient $\beta(z) \geqslant \beta_0$ is a piecewise smooth function, i.e.

$$\beta(z) = \begin{cases} \beta^-(z) & \text{if } z \in \Omega^-, \\ \beta^+(z) & \text{if } z \in \Omega^+, \end{cases} \tag{2.3}$$

which has a finite jump of function values across the interface Γ. At the interface Γ, one has the following homogeneous jump conditions

$$[u]_\Gamma = u^+ - u^- = 0, \tag{2.4}$$

$$[\beta u_n]_\Gamma = \beta^+ u_n^+ - \beta^- u_n^- = 0, \tag{2.5}$$

where u_n denotes the normal flux $\nabla u \cdot n$ with n as the unit outer normal vector of the interface Γ.

In this paper, we use the standard notations for Sobolev spaces and their associate norms given in (Brenner & Scott, 2008; Ciarlet, 2002; Evans, 2010). For a subdomain A of Ω, let $\mathbb{P}_m(A)$ be the space of polynomials of degree less than or equal to m in A and n_m be the dimension of $\mathbb{P}_m(A)$ which equals to $\frac{1}{2}(m+1)(m+2)$. $W^{k,p}(A)$ denotes the Sobolev space with norm $\|\cdot\|_{k,p,A}$ and seminorm $|\cdot|_{k,p,A}$. When $p = 2$, $W^{k,2}(A)$ is simply denoted by $H^k(A)$ and the subscript p is omitted in its associate norm and seminorm. As in (Wei *et al.*, 2014), denote $W^{k,p}(\Omega^- \cup \Omega^+)$ as the function space consisting of

piecewise Sobolev function w such that $w|_{\Omega^-} \in W^{k,p}(\Omega^-)$ and $w|_{\Omega^+} \in W^{k,p}(\Omega^+)$. For the function space $W^{k,p}(\Omega^- \cup \Omega^+)$, define norm as

$$\|w\|_{k,p,\Omega^- \cup \Omega^+} = \left(\|w\|^p_{k,p,\Omega^-} + \|w\|_{k,p,\Omega^+} \right)^{1/p},$$

and seminorm as

$$|w|_{k,p,\Omega^- \cup \Omega^+} = \left(|w|^p_{k,p,\Omega^-} + |w|_{k,p,\Omega^+} \right)^{1/p}.$$

We assume that $\mathscr{T}_h$ is a shape regular triangulation of Ω with $h = \max_{T \in \mathscr{T}} \operatorname{diam}(T)_h$, and that h is small enough so that the interface Γ never crosses any edge of $\mathscr{T}_h$ more than once. The elements of $\mathscr{T}_h$ can be divided into two categories: regular elements and interface elements. We call an element T interface element if the interface Γ passes the interior of T; otherwise, we call it regular element. If Γ passes two vertices of an element T, we treat the element T as a regular element. Let $\mathscr{T}_h^i$ and $\mathscr{T}_h^r$ denote the set of all interface elements and regular elements, respectively.

Let $\mathscr{N}_h$ and $\mathring{\mathscr{E}}_h$ denote the set of all vertices and interior edges of $\mathscr{T}_h$, respectively. We can divide $\mathring{\mathscr{E}}_h$ into two categories: interface edge $\mathring{\mathscr{E}}_h^i$ and regular edge $\mathring{\mathscr{E}}_h^r$, which are defined by

$$\mathring{\mathscr{E}}_h^i = \{e \in \mathring{\mathscr{E}}_h : \mathring{e} \cap \Gamma \neq \emptyset\}, \ , \mathring{\mathscr{E}}_h^r = \mathring{\mathscr{E}}_h \setminus \mathring{\mathscr{E}}_h^i. \tag{2.6}$$

For any interior edge e, there exist two triangles $T_{e,1}$ and $T_{e,2}$ such that $T_{e,1} \cap T_{e,2} = e$. Denote n_e as the unit normal of e pointing from T_1 to T_2, and define

$$\{u\} = \frac{1}{2} \left(u|_{T_{e,1}} + u|_{T_{e,2}} \right), \tag{2.7}$$

$$[u] = u|_{T_{e,1}} - u|_{T_{e,2}}. \tag{2.8}$$

When no confusion arises the subscript e can be dropped. We also introduce two special function spaces X_h and $X_{h,0}$ as

$$X_h := \left\{ v \in L^2(\Omega) : v|_T \in H^1(T) \, , \, v \text{ is continuous at } \mathscr{N}_h \text{ and across } \mathring{\mathscr{E}}_h^r \right\}, \tag{2.9}$$

$$X_{h,0} = \left\{ v \in X_h : v(z) = 0 \text{ for all } z \in \mathscr{N}_h \cap \partial\Omega \right\}. \tag{2.10}$$

We define a bilinear form $a_h : X_{h,0} \times X_{h,0} \to \mathbb{R}$ as

$$
\begin{aligned}
a_h(v,w) = \sum_{T \in \mathscr{T}_h} \int_T \beta \nabla v \cdot \nabla w \, dx - \sum_{e \in \mathring{\mathscr{E}}_h^i} \int_e \{\beta \nabla v \cdot n_e\} [w] ds + \\
\varepsilon \sum_{e \in \mathring{\mathscr{E}}_h^i} \int_e \{\beta \nabla w \cdot n_e\} [v] ds + \sum_{e \in \mathring{\mathscr{E}}_h^i} \int_e \frac{\sigma_e^0}{|e|} [v][w] ds,
\end{aligned}
\tag{2.11}
$$

where the parameter σ_e^0 is positive and the parameter ε can be arbitrary. Usually, ε takes the value -1, 0, or 1. It is easy to see that a_h is symmetric if $\varepsilon = -1$ and it is nonsymmetric otherwise.

The general variational form (Lin *et al.*, 2015) of (2.1)– (2.5) is to find $u_h \in X_{h,0}$ such that

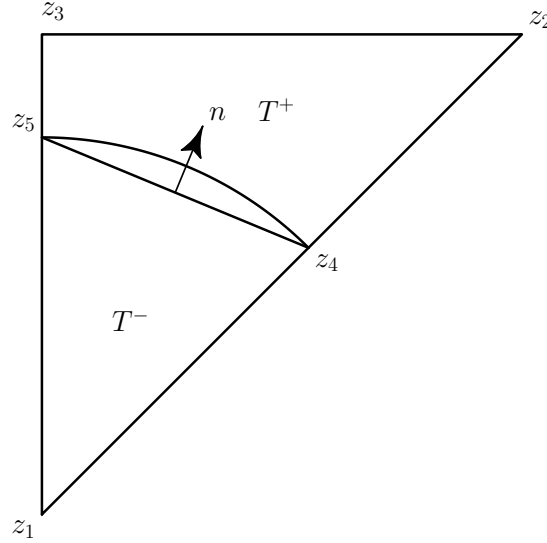$$a_h(u,v) = (f,v), \quad \forall v \in X_{h,0}. \tag{2.12}$$

FIG. 1. Typical example of interface element.

2.2 *Partially penalized immersed finite element method*

The key idea of partially penalized immersed finite element (PPIFE) methods (Lin *et al.*, 2015) is to modify basis functions in interface elements to satisfy jump conditions (2.4) and (2.5). Consider a typical interface element T as in Figure 1, and let z_4 and z_5 be the intersection points between the interface Γ and edges of the element. Connecting the line segment $\overline{z_4 z_5}$ forms an approximation of interface Γ in the element T, denoted by $\Gamma_h|_T$. Then the element T is split into two parts: T^- and T^+. We construct the following piecewise linear function on the interface element T

$$\phi(z) = \begin{cases} \phi^+ = a^+ + b^+ x + c^+ y, & z = (x,y) \in T^+, \\ \phi^- = a^- + b^- x + c^- y, & z = (x,y) \in T^-, \end{cases} \tag{2.13}$$

where the coefficients are determined by the following linear system

$$\phi(z_1) = V_1, \ \phi(z_2) = V_2, \ \phi(z_3) = V_3, \tag{2.14}$$

$$\phi^+(z_4) = \phi^-(z_4), \phi^+(z_5) = \phi^-(z_5), \beta^+ \partial_n \phi^+ = \beta^- \partial_n \phi^-, \tag{2.15}$$

with V_i being the nodal variables. The immersed finite element space V_h (Li *et al.*, 2003) is defined as

$$V_h := \left\{ v \in L^2(\Omega) : v|_T \in V_h(T) \text{ and } v \text{ is continuous on } \mathcal{N}_h, \right\}, \tag{2.16}$$

$$V_{h,0} = \left\{ v \in V_h : v(z) = 0 \text{ for all } z \in \mathcal{N}_h \cap \partial \Omega \right\}, \tag{2.17}$$

where

$$V_h(T) := \begin{cases} \{v | v \in \mathbb{P}_1(T)\}, & \text{if } T \in \mathcal{T}_h^r; \\ \{v | v \text{ is defined by } (2.13) - (2.15)\}, & \text{if } T \in \mathcal{T}_h^i. \end{cases} \tag{2.18}$$

A function in $V_h(T)$ is called a linear IFE function on T when T is an interface element. For the linear IFE function, traditional trace inequality (Brenner & Scott, 2008; Ciarlet, 2002) fails. In (Lin *et al.*, 2015), Lin et al. established the following trace inequality:

LEMMA 2.1 Let *T* be an arbitrary interface element and *e* be an edge of *T*. Then there exists a constant *C* independent of the interface location and mesh size *h* such that the following inequality holds:

$$\|\beta\nabla v \cdot n_e\|_{0,e} \leqslant Ch^{1/2}|T|^{-1/2}\|\sqrt{\beta}\nabla v\|_{0,T}.$$ (2.19)

for every linear IFE function *v* on *T*.

It is obvious that V_h (resp. $V_{h,0}$) is a subspace of X_h (resp. $X_{h,0}$). The PPIFE methods for (2.1)– (2.5) read as finding $u_h \in V_{h,0}$ such that

$$a_h(u_h, v_h) = (f, v_h), \quad \forall v_h \in V_{h,0}.$$ (2.20)

The energy norm $\|\cdot\|_h$ is defined as

$$\|v_h\|_h = \left(\sum_{T \in \mathscr{T}_h} \int_T \beta \nabla v_h \cdot \nabla v_h dx + \sum_{e \in \mathscr{E}_h^i} \int_e \frac{\sigma_e^0}{|e|} [v_h]^2 ds \right)^{1/2}.$$ (2.21)

The following coercivity has been proved in (Lin *et al.*, 2015):

LEMMA 2.2 There exists a constant $C > 0$ such that

$$C\|v_h\|_h^2 \leqslant a_h(v_h, v_h), \quad \forall v_h \in V_{h,0},$$ (2.22)

is true for $\varepsilon = 1$ unconditionally and is true for $\varepsilon = 0$ or $\varepsilon = -1$ under the condition that σ_e^0 is large enough.

Based on the above coercivity, Lin et al. proved the following optimal convergence result:

THEOREM 2.1 Assume that the exact solution *u* to the interface problem (2.1)– (2.5) is in $H^3(\Omega^- \cup \Omega^+)$ and u_h is the solution to (2.20) on a Cartesian mesh $\mathscr{T}_h$. Then there exists a constant *C* such that

$$\|u - u_h\|_h \leqslant Ch\|u\|_{3,\Omega^- \cup \Omega^+}.$$ (2.23)

REMARK 2.1 As remarked in (Lin *et al.*, 2015), when the exact solution belongs to $W^{2,\infty}(\Omega^- \cup \Omega^+)$, the IFE solution u_h of (2.20) on a Cartesian mesh $\mathscr{T}_h$ has error estimation in the following form

$$\|u - u_h\|_h \leqslant C\left(h\|u\|_{2,\Omega^- \cup \Omega^+} + h^{1.5}\|u\|_{2,\infty,\Omega^- \cup \Omega^+}\right).$$ (2.24)

Note that the above error estimation is also an optimal one since the leading (first) term is of $\mathscr{O}(h)$.

3. Superconvergence Analysis

In this section, we first present a superconvergence analysis for the PPIFE method on shape regular meshes. Then we show that the gradient recovery method introduced in (Guo & Yang, 2017) is applicable and prove that the recovered gradient is superconvergent to the exact gradient.

3.1 *Supercloseness result*

From now on, we suppose $\mathscr{T}_h$ is a shape regular triangular mesh although $\mathscr{T}_h$ is usually Cartesian mesh in the literature of IFE methods. Let $h = \max_{T \in \mathscr{T}_h} \text{diam}(T)$. The set of regular element $\mathscr{T}_h^r$ can be further

decomposed into the following two disjoint parts:

$$\mathscr{T}_h^- := \left\{ T \in \mathscr{T}_h^r | T \text{ has all three vertices in } \overline{\Omega^-} \right\},$$
$$\mathscr{T}_h^+ := \left\{ T \in \mathscr{T}_h^r | T \text{ has all three vertices in } \overline{\Omega^+} \right\}. \tag{3.1}$$

DEFINITION 3.1 1. Two adjacent triangles are called to form an $\mathscr{O}(h^{1+\alpha})$ approximate parallelogram if the lengths of any two opposite edges differ only by $\mathscr{O}(h^{1+\alpha})$.

2. The triangulation $\mathscr{T}_h$ is called to satisfy Condition (σ, α) if there exist a partition $\mathscr{T}_{h,1} \cup \mathscr{T}_{h,2}$ of $\mathscr{T}_h$ and positive constants α and σ such that every two adjacent triangles in $\mathscr{T}_{h,1}$ form an $\mathscr{O}(h^{1+\alpha})$ parallelogram and

$$\sum_{T \in \mathscr{T}_{h,2}} |T| = \mathscr{O}(h^{\sigma}).$$

REMARK 3.1 It is obvious that Cartesian mesh satisfies Condition (σ, α) with $\sigma = \infty$ and $\alpha = 1$.

Suppose $\mathscr{T}_h$ satisfies Condition (σ, α). Then we can prove the following supercloseness result:

THEOREM 3.2 Suppose the triangulation $\mathscr{T}_h$ satisfies Condition (σ, α). Let u be the solution of the interface problem (2.1)–(2.5) and u_I be the interpolation of u in the IFE space $V_{h,0}$. If $u \in H^1(\Omega) \cap H^3(\Omega^- \cup \Omega^+) \cap W^{2,\infty}(\Omega^- \cup \Omega^+)$, then for all $v_h \in V_{h,0}$

$$a_h(u - u_I, v_h) \leqslant C \left(h^{1+\rho} (\|u\|_{3,\Omega^+ \cup \Omega^-} + \|u\|_{2,\infty,\Omega^+ \cup \Omega^-}) + Ch^{1.5} \|u\|_{2,\infty,\Omega^+ \cup \Omega^-} \right) \|v_h\|_h. \tag{3.2}$$

where C is a constant independent of interface location and h and $\rho = \min(\alpha, \frac{\sigma}{2}, \frac{1}{2})$.

Proof. Notice that

$$
\begin{aligned}
& a_h(u - u_I, v_h) \\
&= \sum_{T \in \mathscr{T}_h} \int_T \beta \nabla(u - u_I) \cdot \nabla v_h dx - \sum_{e \in \mathscr{E}_h^{\mathring{i}}} \int_e \{\beta \nabla(u - u_I) \cdot n_e\} [v_h] ds + \\
& \quad \varepsilon \sum_{e \in \mathscr{E}_h^{\mathring{i}}} \int_e \{\beta \nabla v_h \cdot n_e\} [u - u_I] ds + \sum_{e \in \mathscr{E}_h^{\mathring{i}}} \int_e \frac{\sigma_e^0}{|e|} [u - u_I][v_h] ds \\
&= \sum_{T \in \mathscr{T}_h^+} \int_T \beta \nabla(u - u_I) \cdot \nabla v_h dx + \sum_{T \in \mathscr{T}_h^-} \int_T \beta \nabla(u - u_I) \cdot \nabla v_h dx \\
& \quad \sum_{T \in \mathscr{T}_h^i} \int_T \beta \nabla(u - u_I) \cdot \nabla v_h dx - \sum_{e \in \mathscr{E}_h^{\mathring{i}}} \int_e \{\beta \nabla(u - u_I) \cdot n_e\} [v_h] ds + \\
& \quad \varepsilon \sum_{e \in \mathscr{E}_h^{\mathring{i}}} \int_e \{\beta \nabla v_h \cdot n_e\} [u - u_I] ds + \sum_{e \in \mathscr{E}_h^{\mathring{i}}} \int_e \frac{\sigma_e^0}{|e|} [u - u_I][v_h] ds \\
&= I_1 + I_2 + I_3 + I_4 + I_5 + I_6.
\end{aligned}
\tag{3.3}
$$

Since $\mathscr{T}_h$ satisfies Condition (σ, α), it follows that $\mathscr{T}_h^+$ and $\mathscr{T}_h^-$ also satisfy the Condition (σ, α). Using the fact that the IFE functions becoming standard linear functions on regular elements, we have

H. GUO *ET AL.*

the following estimates for I_1 and I_2, whose proof can be found in (Xu & Zhang, 2004):

$$|I_1| \leqslant Ch^{1+\rho}(\|u\|_{3,\Omega^+} + \|u\|_{2,\infty,\Omega^+})|v_h|_h, \tag{3.4}$$

$$|I_2| \leqslant Ch^{1+\rho}(\|u\|_{3,\Omega^-} + \|u\|_{2,\infty,\Omega^-})|v_h|_h, \tag{3.5}$$

where C is a constant independent of the location of the interface and mesh size h and $\rho = \min(\alpha, \frac{\sigma}{2}, \frac{1}{2})$.
Now we proceed to estimate I_3. By the Cauchy-Schwartz inequality, we have

$$
\begin{aligned}
I_3 &= \sum_{T \in \mathscr{T}_h^i} \int_T \beta \nabla(u - u_I) \cdot \nabla v_h dx \\
&\leqslant \left(\sum_{T \in \mathscr{T}_h^i} \|\beta^{1/2} \nabla(u - u_I)\|_{0,T}^2 \right)^{1/2} \left(\sum_{T \in \mathscr{T}_h^i} \|\beta^{1/2} \nabla v_h\|_{0,T}^2 \right)^{1/2} \\
&\leqslant \left(\sum_{T \in \mathscr{T}_h^i} \max(\beta^-, \beta^+) \|\nabla(u - u_I)\|_{0,T}^2 \right)^{1/2} \left(\sum_{T \in \mathscr{T}_h^i} \|\beta^{1/2} \nabla v_h\|_{0,T}^2 \right)^{1/2} \\
&\leqslant C \left(\sum_{T \in \mathscr{T}_h^i} h^2 \|u\|_{2,T^- \cup T^+}^2 \right)^{1/2} \left(\sum_{T \in \mathscr{T}_h^i} \|\beta^{1/2} \nabla v_h\|_{0,T}^2 \right)^{1/2} \\
&\leqslant C \left(\sum_{T \in \mathscr{T}_h^i} h^4 \|u\|_{2,\infty,T^- \cup T^+}^2 \right)^{1/2} \left(\sum_{T \in \mathscr{T}_h^i} \|\beta^{1/2} \nabla v_h\|_{0,T}^2 \right)^{1/2} \\
&\leqslant Ch^2 \|u\|_{2,\infty,\Omega^- \cup \Omega^+} \left(\sum_{T \in \mathscr{T}_h^i} 1 \right)^{1/2} \left(\sum_{T \in \mathscr{T}_h^i} \|\beta^{1/2} \nabla v_h\|_{0,T}^2 \right)^{1/2} \\
&\leqslant Ch^{3/2} \|u\|_{2,\infty,\Omega^- \cup \Omega^+} \left(\sum_{T \in \mathscr{T}_h^i} \|\beta^{1/2} \nabla v_h\|_{0,T}^2 \right)^{1/2} \\
&\leqslant Ch^{3/2} \|u\|_{2,\infty,\Omega^- \cup \Omega^+} \|v_h\|_h,
\end{aligned}
\tag{3.6}
$$

where we have used optimal approximation capability of IFE space (Li *et al.*, 2004, 2003) and the fact

that $\sum_{T \in \mathscr{T}_h^i} 1 \approx \mathscr{O}(h^{-1})$. Then we estimate I_4. Cauchy-Schwartz inequality implies that

$$
\begin{aligned}
I_4 &= \sum_{e \in \mathring{\mathscr{E}}_h^i} \int_e \{\beta \nabla(u - u_I) \cdot n_e\}[v_h]ds \\
&\leqslant \left(\sum_{e \in \mathring{\mathscr{E}}_h^i} \int_e \frac{|e|}{\sigma_e^0} \{\beta \nabla(u - u_I) \cdot n_e\}^2 ds \right)^{1/2} \left(\sum_{e \in \mathring{\mathscr{E}}_h^i} \int_e \frac{\sigma_e^0}{|e|}[v_h]^2 ds \right)^{1/2} \\
&\leqslant Ch^{1/2} \left(\sum_{e \in \mathring{\mathscr{E}}_h^i} \int_e \{\beta \nabla(u - u_I) \cdot n_e\}^2 ds \right)^{1/2} \left(\sum_{e \in \mathring{\mathscr{E}}_h^i} \int_e \frac{\sigma_e^0}{|e|}[v_h]^2 ds \right)^{1/2} \\
&\leqslant Ch^2 \|u\|_{2,\infty,\Omega^- \cup \Omega^+} \left(\sum_{T \in \mathscr{T}_h^i} 1 \right)^{1/2} \left(\sum_{e \in \mathring{\mathscr{E}}_h^i} \int_e \frac{\sigma_e^0}{|e|}[v_h]^2 ds \right)^{1/2} \\
&\leqslant Ch^{3/2} \|u\|_{2,\infty,\Omega^- \cup \Omega^+} \|v_h\|_h,
\end{aligned}
\tag{3.7}
$$

where we have used (4.19) in (Lin *et al.*, 2015). To bound I_5, we use the standard trace inequality (Brenner & Scott, 2008; Ciarlet, 2002), since $(u - u_I)|_{T_i}$ is a function in $H^1(T_i)$, and consider only the trace of $u - u_I$, for which we have

$$
\begin{aligned}
\|[u - u_I]\|_{0,e} &\leqslant \|(u - u_I)|_{T_{e,1}}\|_{0,e} + \|(u - u_I)|_{T_{e,2}}\|_{0,e} \\
&\leqslant Ch^{-1/2} \left(\|u - u_I\|_{0,T_{e,1}} + h\|\nabla(u - u_I)\|_{0,T_{e,1}} \right) + \\
&\quad Ch^{-1/2} \left(\|u - u_I\|_{0,T_{e,2}} + h\|\nabla(u - u_I)\|_{0,T_{e,2}} \right) \\
&\leqslant Ch^{3/2} \left(\|u\|_{2,T_{e,1}^- \cup T_{e,1}^+} + \|u\|_{2,T_{e,2}^- \cup T_{e,1}^+} \right) \\
&\leqslant Ch^{3/2} \|u\|_{2,\infty,\Omega^- \cup \Omega^+}.
\end{aligned}
\tag{3.8}
$$

Also, the trace inequality for IFE function (2.19) implies that

$$
\begin{aligned}
\| \{\beta \nabla v_h \cdot n_e\} \|_{0,e} &\leqslant \| \{\beta \nabla v_h|_{T_{e,1}} \cdot n_e\} \|_{0,e} + \| \{\beta \nabla v_h|_{T_{e,2}} \cdot n_e\} \|_{0,e} \\
&\leqslant Ch^{-1/2} \left(\|\sqrt{\beta} \nabla v_h\|_{0,T_{e,1}} + \|\sqrt{\beta} \nabla v_h\|_{0,T_{e,2}} \right).
\end{aligned}
\tag{3.9}
$$

Hence, we get

$$
\begin{aligned}
I_5 &= \left| \varepsilon \sum_{e \in \mathring{\mathcal{E}}_h^i} \int_e \{\beta \nabla v_h \cdot n_e\} [u - u_I] ds \right| \\
&\leqslant \left(\sum_{e \in \mathring{\mathcal{E}}_h^i} \| \{\beta \nabla v_h \cdot n_e\} \|_{0,e}^2 \right)^{1/2} \left(\sum_{e \in \mathring{\mathcal{E}}_h^i} \| [u - u_I] \|_{0,e}^2 \right)^{1/2} \\
&\leqslant C \left(\sum_{e \in \mathring{\mathcal{E}}_h^i} h^{-1} \left(\| \sqrt{\beta} \nabla v_h \|_{0,T_{e,1}} + \| \sqrt{\beta} \nabla v_h \|_{0,T_{e,2}} \right)^2 \right)^{1/2} \left(\sum_{e \in \mathring{\mathcal{E}}_h^i} h^5 \| u \|_{2,\infty,\Omega^- \cup \Omega^+}^2 \right)^{1/2} \\
&\leqslant C h^2 \| u \|_{2,\infty,\Omega^- \cup \Omega^+} \left(\sum_{T \in \mathscr{T}_h^i} \| \sqrt{\beta} \nabla v_h \|_{0,T}^2 \right)^{1/2} \left(\sum_{T \in \mathscr{T}_h^i} 1 \right)^{1/2} \\
&\leqslant C h^{3/2} \| u \|_{2,\infty,\Omega^- \cup \Omega^+} \| v_h \|_h,
\end{aligned}
\tag{3.10}
$$

where we have also used the fact $\sum_{T \in \mathscr{T}_h^i} 1 \approx \mathcal{O}(h^{-1})$. For I_6, by the Cauchy-Schwartz inequality and (3.8), we have

$$
\begin{aligned}
I_6 &= \sum_{e \in \mathring{\mathcal{E}}_h^i} \int_e \frac{\sigma_e^0}{|e|} [u - u_I][v_h] ds \\
&\leqslant \left(\sum_{e \in \mathring{\mathcal{E}}_h^i} \int_e \frac{\sigma_e^0}{|e|} [u - u_I]^2 ds \right)^{1/2} \left(\sum_{e \in \mathring{\mathcal{E}}_h^i} \int_e \frac{\sigma_e^0}{|e|} [v_h]^2 ds \right)^{1/2} \\
&\leqslant C h^{-1/2} \left(\sum_{e \in \mathring{\mathcal{E}}_h^i} \| [u - u_I] \|_{0,e}^2 \right)^{1/2} \| v_h \|_h \\
&\leqslant C h^2 \| u \|_{2,\infty,\Omega^- \cup \Omega^+} \left(\sum_{T \in \mathscr{T}_h^i} 1 \right)^{1/2} \| v_h \|_h \\
&\leqslant C h^{3/2} \| u \|_{2,\infty,\Omega^- \cup \Omega^+} \| v_h \|_h,
\end{aligned}
\tag{3.11}
$$

where we have also used the fact $\sum_{T \in \mathscr{T}_h^i} 1 \approx \mathcal{O}(h^{-1})$. Summarizing the bounds for I_i ($i = 1, 2, \cdots, 6$) together gives (3.2). $\qquad \square$

REMARK 3.2 When the discontinuity disappears, $\mathring{\mathcal{E}}_h^i$ will become empty. In that case, I_i (i = 3, 4, 5, 6) will become zero and we can reproduce the standard supercloseness result (Xu & Zhang, 2004).

REMARK 3.3 Here we only discuss the triangle element. For the bilinear PPIFE methods, we can prove similar supercloseness results by adapting the integral identities in (Lin *et al.*, 1991; Lin & Yan, 1996), the trace inequalities for bilinear IFE functions (Lin *et al.*, 2015), and the same techniques that we used here to deal with the interface part.

Based on the supercloseness results, we can prove the following theorem:

THEOREM 3.3 Assume the same hypothesis in Theorem 3.2 and let u_h be the IFE solution of discrete variational problem (2.20) ; then

$$\|u_h - u_I\|_h \leqslant C \left(h^{1+\rho}(\|u\|_{3,\Omega^+\cup\Omega^-} + \|u\|_{2,\infty,\Omega^+\cup\Omega^-}) + Ch^{3/2}\|u\|_{2,\infty,\Omega^+\cup\Omega^-} \right), \qquad (3.12)$$

where $\rho = \min(\alpha, \frac{\sigma}{2}, \frac{1}{2})$.

Proof. Since $V_{h,0}$ is a subset of $X_{h,0}$, it follows that

$$a_h(u - u_h, v_h) = 0, \quad \forall v_h \in V_{h,0}. \qquad (3.13)$$

Then we have

$$a_h(u_h - u_I, v_h) = a_h(u - u_I, v_h), \quad \forall v_h \in V_{h,0}. \qquad (3.14)$$

Taking $v_h = u_h - u_I$ and using Theorem 3.2 and Lemma 2.2, we prove (3.12). □

REMARK 3.4 Similarly as Remark 3.2, when the discontinuity disappears, (3.12) will reduce to the standard supercloseness result (Xu & Zhang, 2004).

3.2 *Superconvergence results*

In this subsection, using the supercloseness results, we show that the recovered gradient of the PPIFE solution is superconvergent to the exact gradient.

To define the gradient recovery operator introduced (Guo & Yang, 2017), we first generate a local body-fitted mesh $\widehat{\mathcal{T}_h}$, by adding some new vertices into $\mathcal{N}_h$ (Guo & Yang, 2017; Li *et al.*, 2003). Here the body-fitted mesh means that the triangulation $\widehat{\mathcal{T}_h}$ is aligned with the interface, assuming that $\widehat{S}_h$ is the C^0 linear finite element space defined on $\widehat{\mathcal{T}_h}$.

Let $\widehat{\mathcal{N}_h}$ denote all vertices in $\widehat{\mathcal{T}_h}$, and one has $\mathcal{N}_h \subset \widehat{\mathcal{N}_h}$. For any $z \in \widehat{\mathcal{N}_h}$, let $\widehat{\mathcal{T}_z}$ denote the set of all triangles in $\widehat{\mathcal{T}_h}$ having z as their vertex and define

$$(E_h v)(z) = \frac{1}{|\widehat{\mathcal{T}_z}|} \sum_{\widehat{T} \in \widehat{\mathcal{T}_z}} v_{\widehat{T}}(z), \qquad (3.15)$$

with $|\widehat{\mathcal{T}_z}|$ being the cardinality of $\widehat{\mathcal{T}_z}$ and $v_{\widehat{T}} = v|_{\widehat{T}}$. We can define $E_h v$ on Ω by standard linear finite element interpolation in $\widehat{S}_h$ after obtaining the values $(E_h v)(z)$ at all vertices.

Let Γ_h be the approximated interface by connecting the intersection points of edges with Γ. We can category the triangulation $\widehat{\mathcal{T}_h}$ into the following two disjoint sets:

$$\widehat{\mathcal{T}_h^-} := \left\{ T \in \mathcal{T}_h | \text{ all three vertices of } T \text{ are in } \overline{\Omega^-} \right\}, \qquad (3.16)$$

$$\widehat{\mathcal{T}_h^+} := \left\{ T \in \mathcal{T}_h | \text{ all three vertices of } T \text{ are in } \overline{\Omega^+} \right\}. \qquad (3.17)$$

Let $\Omega_h^- = \cup_{T \in \widehat{\mathcal{T}_h^-}} T$ and $\Omega_h^+ = \cup_{T \in \widehat{\mathcal{T}_h^+}} T$. Suppose $\widehat{S}_h^-$ and $\widehat{S}_h^+$ are the continuous linear finite element spaces defined on $\widehat{\mathcal{T}_h^-}$ and $\widehat{\mathcal{T}_h^+}$, respectively.

Denote the PPR gradient recovery operator on $\widehat{S}_h^-$ by G_h^- (Zhang & Naga, 2005). Note that $G_h^- v_h^-$ is a finite element vector-valued function in $\widehat{S}_h^- \times \widehat{S}_h^-$ for any given finite element function $v_h^- \in \widehat{S}_h^-$. To define the recovered gradient $G_h^- v_h^-$, it suffices to define $G_h^- v_h^-$ at every nodal point. Let $\widehat{\mathcal{N}_h^-}$ denote the set of all nodal point of $\widehat{\mathcal{T}_h^-}$. For any vertex $z \in \widehat{\mathcal{N}_h^-}$, let $\widehat{\mathcal{K}_z^-}$ be a patch of elements in $\widehat{\mathcal{T}_h^-}$ around z. The readers are referred to (Zhang & Naga, 2005; Naga & Zhang, 2004; Guo *et al.*, 2016) for the construction of the local patch of elements $\widehat{\mathcal{K}_z^-}$. Select all nodes in $\widehat{\mathcal{N}_h^-} \cap \widehat{\mathcal{K}_z^-}$ as sampling points and fit a polynomial $p_z \in \mathbb{P}_{k+1}(\widehat{\mathcal{K}_z^-})$ in the least square sense at those sampling points, i.e.

$$p_z = \arg \min_{p \in \mathbb{P}_{k+1}(\widehat{\mathcal{K}_z^-})} \sum_{\tilde{z} \in \widehat{\mathcal{N}_h^-} \cap \widehat{\mathcal{K}_z^-}} (u_h - p)^2(\tilde{z}). \tag{3.18}$$

Then the recovered gradient at z is defined as

$$(G_h^- u_h)(z) = \nabla p_z(z).$$

The gradient recovery operator G_h^- is a bounded operator in the sense of

$$\|G_h^- v_h^-\|_{0,\Omega} \leqslant C |v^-|_{0,\Omega^-}, \tag{3.19}$$

with C being a constant independent of the mesh size h and the solution u.

Similarly, we can define the PPR gradient recovery operator G_h^+ from $\widehat{S}_h^+$ to $\widehat{S}_h^+ \times \widehat{S}_h^+$. Then, for any $u_h \in V_h$, let $G_h^I : \widehat{S}_h \to (\widehat{S}_h^- \cup \widehat{S}_h^+) \times (\widehat{S}_h^- \cup \widehat{S}_h^+)$ be the improved polynomial preserving recovery (IPPR) operator proposed in (Guo & Yang, 2016a) which is defined as following.

$$(G_h^I u_h)(z) = \begin{cases} (G_h^- u_h)(z) & \text{if } z \in \overline{\Omega_h^-}, \\ (G_h^+ u_h)(z) & \text{if } z \in \overline{\Omega_h^+}. \end{cases} \tag{3.20}$$

Then the recovered gradient of PPIFE solution u_h is defined as

$$R_h u_h = G_h^I(E_h v_h). \tag{3.21}$$

The linear boundedness and consistency of the gradient recovery operator R_h are showed in (Guo & Yang, 2017). The previous established supercloseness result enables us to prove the following main superconvergence result:

THEOREM 3.4 Assume the same hypothesis in Theorem 3.2 and let u_h be the IFE solution of discrete variational problem (2.20) ; then

$$\|\nabla u - R_h u_h\|_{0,\Omega} \leqslant C \left(h^{1+\rho}(\|u\|_{3,\Omega^+ \cup \Omega^-} + \|u\|_{2,\infty,\Omega^+ \cup \Omega^-}) + Ch^{1.5}\|u\|_{2,\infty,\Omega^+ \cup \Omega^-} \right). \tag{3.22}$$

Proof. We decompose $\nabla u - R_h u_h$ as $(\nabla u - R_h u_I) - (R_h u_I - R_h u_h)$. Then the triangle inequality implies that

$$\|\nabla u - R_h u_h\|_{0,\Omega} \leqslant \|\nabla u - R_h u_I\|_{0,\Omega} + \|R_h u_I - R_h u_h\|_{0,\Omega} := I_1 + I_2. \tag{3.23}$$

According to Theorem 3.7 in (Guo & Yang, 2017), we have

$$I_1 \lesssim h^2 \|u\|_{3,\Omega^- \cup \Omega^+}. \tag{3.24}$$

Using definition (3.21), we obtain that

$$
\begin{aligned}
I_2 &= \|G_h E_h(u_I - u_h)\|_{0,\Omega} \\
&\lesssim \|G_h^- E_h(u_I - u_h)\|_{0,\Omega_h^-} + \|G_h^+ E_h(u_I - u_h)\|_{0,\Omega_h^+} \\
&\lesssim \|\nabla E_h(u_I - u_h)\|_{0,\Omega_h^-} + \|\nabla E_h(u_I - u_h)\|_{0,\Omega_h^+} \\
&\lesssim \|\nabla E_h(u_I - u_h)\|_{0,\Omega} \\
&\lesssim \|\nabla(u_I - u_h)\|_{0,\Omega} \\
&\lesssim h^{1+\rho}(\|u\|_{3,\Omega^+ \cup \Omega^-} + \|u\|_{2,\infty,\Omega^+ \cup \Omega^-}) + Ch^{3/2}\|u\|_{2,\infty,\Omega^+ \cup \Omega^-}
\end{aligned}
\tag{3.25}
$$

where we have used the boundedness property of $G_h^\pm$ in the second inequality, Corollary 3.4 of (Guo & Yang, 2017) in the fourth inequality, and Theorem 3.3 in the last inequality. Combining (3.23)-(3.25) completes the proof of (3.22). □

The gradient recovery operator R_h naturally provides an *a posteriori* error estimators for the PPIFE method. We define a local *a posteriori* error estimator on element $T \in \mathscr{T}_h$ as

$$
\eta_T = \begin{cases}
\|\beta^{1/2}(R_h u_h - \nabla u_h)\|_{0,T}, & \text{if } T \in \mathscr{T}_h^r, \\
\left(\displaystyle\sum_{\widehat{T} \subset T, \widehat{T} \in \widehat{\mathscr{T}_h}} \|\beta^{1/2}(R_h u_h - \nabla u_h)\|_{0,\widehat{T}}^2 \right)^{\frac{1}{2}}, & \text{if } T \in \mathscr{T}_h^i,
\end{cases}
\tag{3.26}
$$

and the corresponding global error estimator as

$$
\eta_h = \left(\sum_{T \in \mathscr{T}_h} \eta_T^2 \right)^{1/2}.
\tag{3.27}
$$

With the above superconvergence result, we are ready to prove the asymptotic exactness of error estimators based on the recovery operator R_h.

THEOREM 3.5 Assume the same hypothesis in Theorem 3.2 and let u_h be the IFE solution of discrete variational problem (2.20). Further assume that there is a constant $C(u) > 0$ such that

$$
\|\nabla(u - u_h)\|_{0,\Omega} \geqslant C(u)h.
\tag{3.28}
$$

Then it holds that

$$
\left| \frac{\eta_h}{\|\beta^{1/2}\nabla(u - u_h)\|_{0,\Omega}} - 1 \right| \leqslant Ch^\rho.
\tag{3.29}
$$

Proof. By the Triangle inequality, Theorem 3.4, and (3.28), we have

$$
\left| \frac{\eta_h}{\|\beta^{1/2}\nabla(u - u_h)\|_{0,\Omega}} - 1 \right| \leqslant \frac{\|\beta^{1/2}(R_h u_h - \nabla u_h)\|_{0,\Omega}}{\|\beta^{1/2}\nabla(u - u_h)\|_{0,\Omega}} \leqslant \frac{Ch^{1+\rho}\left(\|u\|_{3,\Omega^+ \cup \Omega^-} + \|u\|_{2,\infty,\Omega^+ \cup \Omega^-}\right)}{\min(\beta^+, \beta^-)c(u)h} \leqslant Ch^\rho.
$$

□

REMARK 3.5 Assumption 3.28 is reasonable on general shape regular meshes by the lower bounds of the approximation error by piecewise polynomials (Lin *et al.*, 2014).

REMARK 3.6 Theorem 3.5 implies that (3.26) (or (3.27)) is an asymptotically exact *a posteriori* error estimator for PPIFE methods.

4. Numerical Examples

In the section, the previously established supercloseness and superconvergence theory are demonstrated by three numerical examples. The first two are benchmark problems for testing numerical methods for linear interface problem. For that two examples, the computational domain are chosen as $\Omega = [-1,1] \times [-1,1]$. The uniform triangulation of Ω is obtained by dividing Ω into N^2 sub-squares and then dividing each sub-square into two right triangles. The resulting uniform mesh size is $h = 1/N$. The last example is a nonlinear interface problem. We test the examples using three different PPIFE methods (Lin *et al.*, 2015): the symmetric PPIFE method (SPPIFEM), incomplete PPIFE method (IPPIFEM), and non-symmetric PPIFE method (NPPIFEM), which are corresponding to $\varepsilon = -1$, $\varepsilon = 0$, and $\varepsilon = 1$, respectively. We choose the penalty parameter $\sigma_e^0 = \sqrt{\max(\beta^-, \beta^+)}$ for SPPIFEM and IPPIFEM and $\sigma_e^0 = 1$ for NPPIFEM. For convenience, we shall adopt the following error norms in all the examples:

$$De := \|\nabla(u - u_h)\|_{0,\Omega}, \quad D^i e := \|\nabla u_I - \nabla u_h\|_{0,\Omega}, \quad D^r e := \|\nabla u - R_h u_h\|_{0,\Omega}. \tag{4.1}$$

Example 4.1. In this example, we consider the elliptic interface problem (2.1) with a circular interface of radius $r_0 = \frac{\pi}{6}$ as studied in (Li *et al.*, 2003). The exact solution is

$$u(z) = \begin{cases} \frac{r^3}{\beta^-} & \text{if } z \in \Omega_-, \\ \frac{r^3}{\beta^+} + \left(\frac{1}{\beta^-} - \frac{1}{\beta^+}\right) r_0^3 & \text{if } z \in \Omega^+, \end{cases}$$

where $r = \sqrt{x^2 + y^2}$.

We use two typical jump ratios: $\beta^-/\beta^+ = 1/10$ and $\beta^-/\beta^+ = 1/1000$. Tables 1-6 report numerical results. For De, all three partially penalized finite element methods converge with the optimal rate $\mathcal{O}(h)$ for both differential jump ratios. As for $D^i e$ and $D^r e$, $\mathcal{O}(h^{1.5})$ order of convergence can be clearly observed for all cases, which support our Theorems 3.3 and 3.4.

We also test the case with jump ratio $\beta^-/\beta^+ = 1/1000000$. The numerical result for SPPIFEM is listed in Table 7. The supercloseness result and superconvergent rate can be also observed in Table 7.

Table 1. SPPIFEM for Example 4.1 with $\beta^+ = 10, \beta^- = 1$.

h	De	order	$D^i e$	order	$D^r e$	order
1/16	7.20e-02	–	3.64e-03	–	1.91e-02	–
1/32	3.62e-02	0.99	1.34e-03	1.44	5.10e-03	1.91
1/64	1.81e-02	1.00	4.64e-04	1.53	1.68e-03	1.60
1/128	9.07e-03	1.00	1.58e-04	1.56	5.24e-04	1.68
1/256	4.53e-03	1.00	5.76e-05	1.45	1.71e-04	1.62
1/512	2.27e-03	1.00	2.00e-05	1.53	5.87e-05	1.54
1/1024	1.13e-03	1.00	7.07e-06	1.50	1.94e-05	1.60

Example 4.2. In this example, we consider the interface problem (2.1) with a cardioid interface as in (Hou & Liu, 2005). The interface curve Γ is the zero level of the function

$$\phi(x,y) = (3(x^2 + y^2) - x)^2 - x^2 - y^2,$$

as shown Figure 2. We choose the exact solution $u(x,y) = \phi(x,y)/\beta(x,y)$, where

$$\beta(x,y) = \begin{cases} xy + 3 & \text{if } (x,y) \in \Omega^-, \\ 100 & \text{if } (x,y) \in \Omega^+. \end{cases}$$

Table 2. IPPIFEM for Example 4.1 with $\beta^+ = 10, \beta^- = 1$.

h	De	order	$D^i e$	order	$D^r e$	order
1/16	7.20e-02	–	3.61e-03	–	1.90e-02	–
1/32	3.62e-02	0.99	1.22e-03	1.57	5.01e-03	1.92
1/64	1.81e-02	1.00	3.98e-04	1.62	1.63e-03	1.62
1/128	9.07e-03	1.00	1.38e-04	1.53	5.07e-04	1.68
1/256	4.53e-03	1.00	4.94e-05	1.48	1.64e-04	1.63
1/512	2.27e-03	1.00	1.72e-05	1.52	5.58e-05	1.55
1/1024	1.13e-03	1.00	6.05e-06	1.51	1.83e-05	1.61

Table 3. NPPIFEM for Example 4.1 with $\beta^+ = 10, \beta^- = 1$.

h	De	order	$D^i e$	order	$D^r e$	order
1/16	7.20e-02	–	3.90e-03	–	1.89e-02	–
1/32	3.62e-02	0.99	1.29e-03	1.59	4.97e-03	1.93
1/64	1.81e-02	1.00	4.18e-04	1.63	1.59e-03	1.64
1/128	9.07e-03	1.00	1.44e-04	1.53	4.97e-04	1.68
1/256	4.53e-03	1.00	5.17e-05	1.48	1.60e-04	1.64
1/512	2.27e-03	1.00	1.80e-05	1.52	5.43e-05	1.56
1/1024	1.13e-03	1.00	6.34e-06	1.51	1.77e-05	1.61

Table 4. SPPIFEM for Example 4.1 with $\beta^+ = 1000, \beta^- = 1$.

h	De	order	$D^i e$	order	$D^r e$	order
1/16	2.47e-02	–	4.60e-03	–	1.33e-02	–
1/32	1.31e-02	0.91	1.78e-03	1.37	3.62e-03	1.88
1/64	6.56e-03	1.00	6.44e-04	1.47	1.36e-03	1.42
1/128	3.31e-03	0.99	2.17e-04	1.57	4.60e-04	1.56
1/256	1.65e-03	1.01	7.70e-05	1.49	1.38e-04	1.73
1/512	8.23e-04	1.00	2.72e-05	1.50	4.71e-05	1.55
1/1024	4.12e-04	1.00	9.60e-06	1.50	1.59e-05	1.57

Table 5. IPPIFEM for Example 4.1 with $\beta^+ = 1000, \beta^- = 1$.

h	De	order	$D^i e$	order	$D^r e$	order
1/16	2.54e-02	–	8.58e-03	–	1.50e-02	–
1/32	1.35e-02	0.91	3.86e-03	1.15	4.99e-03	1.58
1/64	6.65e-03	1.02	1.29e-03	1.58	1.79e-03	1.48
1/128	3.33e-03	1.00	4.36e-04	1.57	5.46e-04	1.72
1/256	1.65e-03	1.01	1.55e-04	1.50	1.83e-04	1.58
1/512	8.25e-04	1.00	5.60e-05	1.47	6.61e-05	1.46
1/1024	4.12e-04	1.00	2.01e-05	1.48	2.38e-05	1.48

Note that the interface is not Lipschitz-continuous and has a singular point at the origin. Tables 8-10

Table 6. NPPIFEM for Example 4.1 with $\beta^+ = 1000, \beta^- = 1$.

h	De	order	$D^i e$	order	$D^r e$	order
1/16	2.56e-02	–	9.39e-03	–	1.55e-02	–
1/32	1.36e-02	0.91	4.29e-03	1.13	5.34e-03	1.54
1/64	6.67e-03	1.03	1.41e-03	1.61	1.88e-03	1.50
1/128	3.34e-03	1.00	4.84e-04	1.54	5.65e-04	1.74
1/256	1.65e-03	1.01	1.72e-04	1.49	1.95e-04	1.53
1/512	8.25e-04	1.00	6.30e-05	1.45	7.23e-05	1.43
1/1024	4.12e-04	1.00	2.29e-05	1.46	2.67e-05	1.44

Table 7. SPPIFEM for Example 4.1 with $\beta^+ = 1000000, \beta^- = 1$.

Dof	De	order	$D^i e$	order	$D^r e$	order
1/16	3.80e-02	–	2.84e-02	–	3.83e-02	–
1/32	2.03e-02	0.91	1.01e-02	1.49	1.12e-02	1.78
1/64	1.04e-02	0.97	3.51e-03	1.52	4.56e-03	1.29
1/128	5.26e-03	0.98	1.08e-03	1.70	2.29e-03	1.00
1/256	2.65e-03	0.99	3.52e-04	1.62	5.09e-04	2.17
1/512	1.33e-03	0.99	1.32e-04	1.42	1.73e-04	1.56
1/1024	6.65e-04	1.00	4.57e-05	1.52	5.93e-05	1.55

display the numerical data. We observe the same supercloseness and superconvergence phenomena as predicted by our theory.

Table 8. SPPIFEM for Example 4.2 .

h	De	order	$D^i e$	order	$D^r e$	order
1/16	5.77e-02	–	5.71e-03	–	2.48e-02	–
1/32	3.03e-02	0.93	2.39e-03	1.26	7.88e-03	1.66
1/64	1.51e-02	1.01	8.55e-04	1.48	2.27e-03	1.80
1/128	7.43e-03	1.02	3.07e-04	1.48	7.10e-04	1.68
1/256	3.71e-03	1.00	1.13e-04	1.45	2.36e-04	1.59
1/512	1.86e-03	1.00	3.94e-05	1.52	8.84e-05	1.41
1/1024	9.32e-04	1.00	1.39e-05	1.50	3.08e-05	1.52

Example 4.3. In this example, we consider the following nonlinear interface problem

$$-\nabla \cdot (\beta(z)\nabla u(z)) + \sin(u(z)) = f(z), \quad z \text{ in } \Omega \setminus \Gamma,$$

with homogeneous jump conditions (2.4) and (2.5) where $\Omega = [-2,2] \times [-2,2] \setminus [-0.5,0.5] \times [-0.5,0.5]$. The interface curve Γ is circle centered at origin with radius $r_0 = \pi/3$. The exact solution is

$$u(z) = \begin{cases} \frac{\log(r)}{\beta^-}, & \text{if } z \in \Omega_-, \\ \frac{\log(r)}{\beta^+} + \left(\frac{1}{\beta^-} - \frac{1}{\beta^+}\right)\log(r_0), & \text{if } z \in \Omega^+, \end{cases}$$
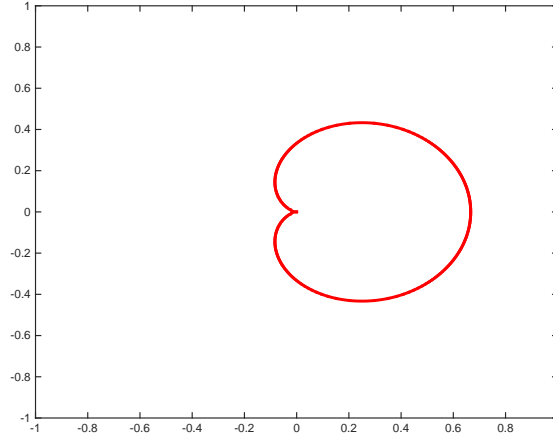
FIG. 2. Shape of interface for Example 4.2

Table 9. IPPIFEM for Example 4.2.

h	De	order	$D^i e$	order	$D^r e$	order
1/16	5.77e-02	–	6.45e-03	–	2.46e-02	–
1/32	3.03e-02	0.93	2.67e-03	1.27	7.63e-03	1.69
1/64	1.51e-02	1.01	9.68e-04	1.46	2.25e-03	1.76
1/128	7.43e-03	1.02	3.55e-04	1.45	6.98e-04	1.69
1/256	3.71e-03	1.00	1.25e-04	1.51	2.30e-04	1.60
1/512	1.86e-03	1.00	4.39e-05	1.51	8.51e-05	1.43
1/1024	9.32e-04	1.00	1.54e-05	1.51	2.95e-05	1.53

Table 10. NPPIFEM for Example 4.2.

h	De	order	$D^i e$	order	$D^r e$	order
1/16	5.78e-02	–	7.96e-03	–	2.47e-02	–
1/32	3.03e-02	0.93	3.12e-03	1.35	7.58e-03	1.70
1/64	1.51e-02	1.01	1.17e-03	1.41	2.29e-03	1.72
1/128	7.43e-03	1.02	4.35e-04	1.43	7.16e-04	1.68
1/256	3.71e-03	1.00	1.51e-04	1.53	2.35e-04	1.61
1/512	1.86e-03	1.00	5.31e-05	1.50	8.62e-05	1.45
1/1024	9.32e-04	1.00	1.87e-05	1.51	3.00e-05	1.52

where $r = |z| = \sqrt{x^2 + y^2}$. The right hand side function f and boundary condition are obtained from the exact solution.

The nonlinear interface problem is solved by the PPIFE method with Newton's iteration on a series of uniform meshes. The coarsest mesh is depicted in Fig 3 and the finer meshes are obtained by the uniform refinement. Numerical results are reported in Tables 11-13. We observe the same superconvergence and supercloseness phenomena as linear problems.
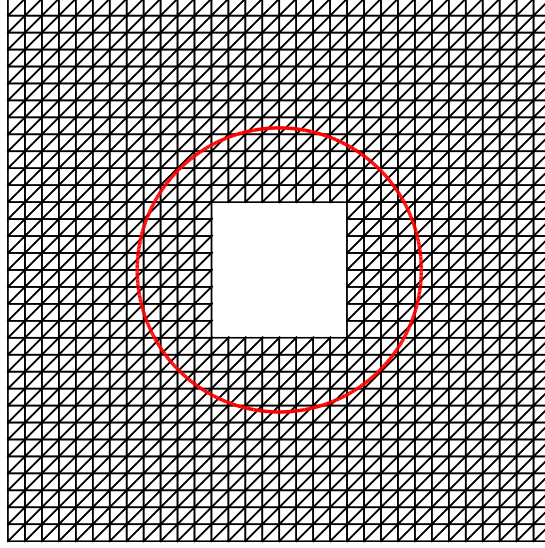
FIG. 3. Initial non body-fitted mesh for Example 4.3

Table 11. SPPIFEM for Example 4.3 with $\beta^+ = 1000, \beta^- = 1$.

h	De	order	$D^i e$	order	$D^r e$	order
1/8	1.69e-01	–	2.55e-02	–	6.44e-02	–
1/16	8.53e-02	0.99	8.54e-03	1.58	1.60e-02	2.01
1/32	4.19e-02	1.03	3.03e-03	1.49	6.13e-03	1.38
1/64	2.09e-02	1.00	1.05e-03	1.53	2.17e-03	1.50
1/128	1.04e-02	1.01	3.70e-04	1.51	6.69e-04	1.70
1/256	5.17e-03	1.00	1.28e-04	1.54	2.34e-04	1.51
1/512	2.58e-03	1.00	4.46e-05	1.52	7.90e-05	1.57

Table 12. IPPIFEM for Example 4.3 with $\beta^+ = 1000, \beta^- = 1$.

h	De	order	$D^i e$	order	$D^r e$	order
1/8	1.75e-01	–	5.15e-02	–	7.52e-02	–
1/16	8.71e-02	1.00	1.90e-02	1.44	2.32e-02	1.70
1/32	4.23e-02	1.04	6.15e-03	1.63	8.27e-03	1.49
1/64	2.10e-02	1.01	1.97e-03	1.64	2.49e-03	1.73
1/128	1.04e-02	1.01	6.85e-04	1.52	8.61e-04	1.53
1/256	5.17e-03	1.01	2.42e-04	1.50	3.17e-04	1.44
1/512	2.58e-03	1.00	8.77e-05	1.47	1.14e-04	1.47

5. Conclusion

In this paper, we study the superconvergence theory for partially penalized immersed finite element (PPIFE) methods. Specifically, we obtain supercloseness results analogous to standard linear finite

Table 13. NPPIFEM for Example 4.3 with $\beta^+ = 1000, \beta^- = 1..$

h	De	order	$D^i e$	order	$D^r e$	order
1/8	1.77e-01	–	6.03e-02	–	8.06e-02	–
1/16	8.78e-02	1.01	2.23e-02	1.44	2.55e-02	1.66
1/32	4.24e-02	1.05	6.89e-03	1.69	8.73e-03	1.55
1/64	2.10e-02	1.01	2.25e-03	1.62	2.63e-03	1.73
1/128	1.04e-02	1.02	7.84e-04	1.52	9.28e-04	1.50
1/256	5.17e-03	1.01	2.80e-04	1.49	3.47e-04	1.42
1/512	2.58e-03	1.00	1.02e-04	1.45	1.29e-04	1.43

element method. Due to the existence of the interface, we can only prove a supercloseness result of order $\mathscr{O}(h^{1.5})$. We also notice that the supercloseness result will reduce to the well-known one for the standard linear element when the discontinuity disappears. These results provide us a fundamental tool to prove the $\mathscr{O}(h^{1.5})$ superconvergence of recovered gradient by using the gradient recovery operator proposed in (Guo & Yang, 2017). We present three numerical examples to support our theoretical results.

Funding

REFERENCES

BABUŠKA, I. (1970) The finite element method for elliptic equations with discontinuous coefficients. *Computing (Arch. Elektron. Rechnen)*, **5**, 207–213.

BABUŠKA, I. & STROUBOULIS, T. (2001) *The finite element method and its reliability*. Numerical Mathematics and Scientific Computation. The Clarendon Press, Oxford University Press, New York, pp. xii+802.

BANK, R. E. & XU, J. (2003) Asymptotically exact a posteriori error estimators. I. Grids with superconvergence. *SIAM J. Numer. Anal.*, **41**, 2294–2312 (electronic).

BARRETT, J. W. & ELLIOTT, C. M. (1987) Fitted and unfitted finite-element methods for elliptic equations with smooth interfaces. *IMA J. Numer. Anal.*, **7**, 283–300.

BASTIAN, P. & ENGWER, C. (2009) An unfitted finite element method using discontinuous Galerkin. *Internat. J. Numer. Methods Engrg.*, **79**, 1557–1576.

BRAMBLE, J. H. & KING, J. T. (1996) A finite element method for interface problems in domains with smooth boundaries and interfaces. *Adv. Comput. Math.*, **6**, 109–138 (1997).

BRENNER, S. C. & SCOTT, L. R. (2008) *The mathematical theory of finite element methods*. Texts in Applied Mathematics, vol. 15, third edn. Springer, New York, pp. xviii+397.

CAI, Z. & ZHANG, S. (2009) Recovery-based error estimator for interface problems: conforming linear elements. *SIAM J. Numer. Anal.*, **47**, 2132–2156.

CAO, W., ZHANG, X. & ZHANG, Z. (2015) Superconvergence of Immersed Finite Element Methods for Interface Problems. arXiv:1511.04648 [math.NA].

CHEN, C. (2001) *Structure Theory of Superconvergence of Finite Elements (in Chinese)*. Hunan Science and Technique Press, Changsha, pp. 1–464.

CHEN, L. & XU, J. (2007) A posteriori error estimator by post-processing. *Adaptive Computations: Theory and Algorithms* (J. Xu & T. Tang eds). Science Press, Beijing, pp. 34–67.

CHEN, Z. & DAI, S. (2002) On the efficiency of adaptive finite element methods for elliptic problems with discontinuous coefficients. *SIAM J. Sci. Comput.*, **24**, 443–462 (electronic).

CHEN, Z. & ZOU, J. (1998) Finite element methods and their convergence for elliptic and parabolic interface problems. *Numer. Math.*, **79**, 175–202.

CHOU, S.-H., KWAK, D. Y. & WEE, K. T. (2010) Optimal convergence analysis of an immersed interface finite element method. *Adv. Comput. Math.*, **33**, 149–168.

CHOU, S.-H. (2012) An immersed linear finite element method with interface flux capturing recovery. *Discrete Contin. Dyn. Syst. Ser. B*, **17**, 2343–2357.

CHOU, S. H. & ATTANAYAKE, C. (2017) Flux recovery and superconvergence of quadratic immersed interface finite elements. *Int. J. Numer. Anal. Model.*, **14**, 88–102.

CIARLET, P. G. (2002) *The finite element method for elliptic problems*. Classics in Applied Mathematics, vol. 40. Society for Industrial and Applied Mathematics (SIAM), Philadelphia, PA, pp. xxviii+530. Reprint of the 1978 original [North-Holland, Amsterdam; MR0520174 (58 #25001)].

EVANS, L. C. (2010) *Partial differential equations*. Graduate Studies in Mathematics, vol. 19, second edn. American Mathematical Society, Providence, RI, pp. xxii+749.

GONG, Y., LI, B. & LI, Z. (2007/08) Immersed-interface finite-element methods for elliptic interface problems with nonhomogeneous jump conditions. *SIAM J. Numer. Anal.*, **46**, 472–495.

GUO, H., ZHANG, Z. & ZHAO, R. (2017) Hessian recovery for finite element methods. *Math. Comp.*, **86**, 1671–1692.

GUO, H. & YANG, X. (2016a) Gradient recovery for elliptic interface problem: I. body-fitted mesh. arXiv:1607.05898 [math.NA].

GUO, H. & YANG, X. (2017) Gradient recovery for elliptic interface problem: II. Immersed finite element methods. *J. Comput. Phys.*, **338**, 606–619.

GUO, H. & ZHANG, Z. (2015) Gradient recovery for the Crouzeix-Raviart element. *J. Sci. Comput.*, **64**, 456–476.

GUO, H., ZHANG, Z., ZHAO, R. & ZOU, Q. (2016) Polynomial preserving recovery on boundary. *J. Comput. Appl. Math.*, **307**, 119–133.

HANSBO, A. & HANSBO, P. (2002) An unfitted finite element method, based on Nitsche's method, for elliptic interface problems. *Comput. Methods Appl. Mech. Engrg.*, **191**, 5537–5552.

HE, X., LIN, T. & LIN, Y. (2012) The convergence of the bilinear and linear immersed finite element solutions to interface problems. *Numer. Methods Partial Differential Equations*, **28**, 312–330.

HOU, S., SONG, P., WANG, L. & ZHAO, H. (2013) A weak formulation for solving elliptic interface problems without body fitted grid. *J. Comput. Phys.*, **249**, 80–95.

HOU, S. & LIU, X.-D. (2005) A numerical method for solving variable coefficient elliptic equation with interfaces. *J. Comput. Phys.*, **202**, 411–445.

HOU, T. Y., WU, X.-H. & ZHANG, Y. (2004) Removing the cell resonance error in the multiscale finite element method via a Petrov-Galerkin formulation. *Commun. Math. Sci.*, **2**, 185–205.

HUANG, P., WU, H. & XIAO, Y. (2017) An unfitted interface penalty finite element method for elliptic interface problems. *Comput. Methods Appl. Mech. Engrg.*, **323**, 439 – 460.

JI, H., CHEN, J. & LI, Z. (2014) A symmetric and consistent immersed finite element method for interface problems. *J. Sci. Comput.*, **61**, 533–557.

KWAK, D. Y., WEE, K. T. & CHANG, K. S. (2010) An analysis of a broken P_1-nonconforming finite element method for interface problems. *SIAM J. Numer. Anal.*, **48**, 2117–2134.

LAKHANY, A. M., MAREK, I. & WHITEMAN, J. R. (2000) Superconvergence results on mildly structured triangulations. *Comput. Methods Appl. Mech. Engrg.*, **189**, 1–75.

LI, Z. (1998) The immersed interface method using a finite element formulation. *Appl. Numer. Math.*, **27**, 253–267.

LI, Z., LIN, T. & WU, X. (2003) New Cartesian grid methods for interface problems using the finite element formulation. *Numer. Math.*, **96**, 61–98.

LI, Z., LIN, T., LIN, Y. & ROGERS, R. C. (2004) An immersed finite element space and its approximation capability. *Numer. Methods Partial Differential Equations*, **20**, 338–367.

LI, Z. & ITO, K. (2006) *The immersed interface method*. Frontiers in Applied Mathematics, vol. 33. Society for Industrial and Applied Mathematics (SIAM), Philadelphia, PA, pp. xvi+332. Numerical solutions of PDEs involving interfaces and irregular domains.

LIN, Q., YAN, N. & ZHOU, A. (1991) A rectangle test for finite element analysis. *Proc. System Science and System Eng.(Hong Kong), Great Wall Culture Publ. Co. Proc. System Science and System Eng.(Hong Kong), Great Wall Culture Publ. Co.*, pp. 213–216.

LIN, Q. & YAN, N. (1996) The construction and analysis of high efficiency finite element methods (in chinese). *Shijiazhuang: Hebei University Publishers*.

LIN, T., LIN, Y. & ZHANG, X. (2015) Partially penalized immersed finite element methods for elliptic interface problems. *SIAM J. Numer. Anal.*, **53**, 1121–1144.

LIN, Q., XIE, H. & XU, J. (2014) Lower bounds of the discretization error for piecewise polynomials. *Math. Comp.*, **83**, 1–13.

NAGA, A. & ZHANG, Z. (2004) A posteriori error estimates based on the polynomial preserving recovery. *SIAM J. Numer. Anal.*, **42**, 1780–1800 (electronic).

NAGA, A. & ZHANG, Z. (2005) The polynomial-preserving recovery for higher order finite element methods in 2D and 3D. *Discrete Contin. Dyn. Syst. Ser. B*, **5**, 769–798.

OSHER, S. & FEDKIW, R. (2003) *Level set methods and dynamic implicit surfaces*. Applied Mathematical Sciences, vol. 153. Springer-Verlag, New York, pp. xiv+273.

SETHIAN, J. A. (1996) *Level set methods*. Cambridge Monographs on Applied and Computational Mathematics, vol. 3. Cambridge University Press, Cambridge, pp. xviii+218. Evolving interfaces in geometry, fluid mechanics, computer vision, and materials science.

WAHLBIN, L. B. (1995) *Superconvergence in Galerkin finite element methods*. Lecture Notes in Mathematics, vol. 1605. Springer-Verlag, Berlin, pp. xii+166.

WEI, H., CHEN, L., HUANG, Y. & ZHENG, B. (2014) Adaptive mesh refinement and superconvergence for two-dimensional interface problems. *SIAM J. Sci. Comput.*, **36**, A1478–A1499.

WU, H. & ZHANG, Z. (2007) Can we have superconvergent gradient recovery under adaptive meshes? *SIAM J. Numer. Anal.*, **45**, 1701–1722.

XU, J. (1982) Error estimates of the finite element method for the 2nd order elliptic equations with discontinuous coefficients. *J. Xiangtan Univ.*, **1**, 1–5.

XU, J. & ZHANG, Z. (2004) Analysis of recovery type a posteriori error estimators for mildly structured grids. *Math. Comp.*, **73**, 1139–1152 (electronic).

ZHANG, Z. & NAGA, A. (2005) A new finite element gradient recovery method: superconvergence property. *SIAM J. Sci. Comput.*, **26**, 1192–1213 (electronic).

ZHU, Q. & LIN, Q. (1989) *Superconvergence Theory of the Finite Element Method (in Chinese)*. Hunan Science and Technique Press, Changsha, pp. 1–464.

ZIENKIEWICZ, O. C. & ZHU, J. Z. (1992a) The superconvergent patch recovery and a posteriori error estimates. I. The recovery technique. *Internat. J. Numer. Methods Engrg.*, **33**, 1331–1364.

ZIENKIEWICZ, O. C. & ZHU, J. Z. (1992b) The superconvergent patch recovery and a posteriori error estimates. II. Error estimates and adaptivity. *Internat. J. Numer. Methods Engrg.*, **33**, 1365–1382.